Nucleation of Polymer Crystals: The "δ Mystery"

Yi-Kang Lan and An-Chung Su*

Department of Chemical Engineering,
National Tsing Hua University, Hsinchu 30013, Taiwan

Introduction. The nucleation stage in polymer crystallization is poorly understood because of experimental difficulties in studying embryos of limited size and transient lifetime. Previous efforts[1] in the understanding of polymer nucleation were mainly focused on incipient crystals, assuming that nuclei are structurally similar to bulk crystals, only being small in size and hence with significant surface effects. The same assumptions were adopted by Hoffman et al.[2] in the "standard" theory of polymer nucleation that has led to the well-known expression of critical lamellar thickness (beyond which crystal growth is thermodynamically spontaneous) $l^* = C/\Delta T + \delta$, where $C = 2\sigma_e T_m°/\Delta H_f°$ (where σ_e is the fold surface energy, $T_m°$ is the "equilibrium melting temperature" at infinite lamellar thickness, and $\Delta H_f°$ is the heat of fusion at $T_m°$), the supercooling $\Delta T \equiv T_m° - T_c$, whereas δ is an empirically added correction to account for the nonzero l^* value upon extrapolation to $(\Delta T)^{-1} = 0$. The nonvanishing δ value (~4 nm for polyethylene, PE)[2,3] constitutes a significant portion of the incipient crystal thickness l^* (typically[2,3] 20 to 10 nm for PE at $\Delta T \approx 15$ to 40 K, with the lowest value recently reported[4] to be ca. 6 nm at $\Delta T \approx 130$ K) and hence is unlikely an artifact of experimental errors. Hoffman et al.[2,5] attributed the nonzero δ to the weak adsorption of stems at the nucleus surface (with the energy of adsorption much lower than the energy of crystallization by a factor of $\psi \approx 0.1$) upon growth via secondary surface nucleation. This was justified using a counterargument that higher ψ values would theoretically lead to uprising crystal thickness with decreasing T_c (the "δ catastrophe"),[2] which is never observed experimentally. However, it remains disturbing that δ finds no counterpart in the nucleation of atomic or small-molecule crystals.

Although the limited size and transient nature of embryos pose a tremendous challenge to experimental investigations of polymer nucleation, these are to the advantage of molecular dynamics (MD) simulations. With improved computing power over the last two decades, there are significant progresses in the scale of MD simulations that bring the technique much closer to realistic molecular systems since the pioneering work by Sumpter et al.[6] in the 2D MD simulation of a single PE chain. Kavassalis and Sundararajan[7] studied aggregation and folding of a chain in vacuum using a 3D MD box; results indicated a two-stage process in which locally collapsed domains were formed first, followed by coalescence of domains into a large lamella. Fujiwara and Sato[8] also studied chain folding in vacuum, emphasizing on bond orientation order and defects in the folded domain. For a single PE long chain on a solid surface, MD results of Guo et al.[9] indicated that intramolecular van der Waals (vdW) attractions are responsible for chain folding into an ordered lamella. From results of 3D MD calculations for polymer chains in vacuum, Muthukumar et al.[10,11] observed that the aggregation of chain segments gives birth to "baby nuclei", which subsequently diffuse to and crystallographically attached on a pre-existing crystal surface. They further suggested that entropic barriers control the selection of the initial lamellar thickness, whereas the subsequent lamellar thickening is a highly cooperative process requiring the mobility of all chains in the crystal.

In contrast with MD simulations in vacuum (i.e., for polymer aggregation in the vapor state), solution-state studies with incorporation of solvent molecules is limited because of more stringent hardware requirements and longer computing times. By setting up a single 250-mer PE chain in *n*-hexane (ca. 2.2 wt % in concentration), Fujiwara et al.[12] showed that the local collapse of chain segments (typically observed in MD results under vacuum environment) is insignificant; instead, the chain tends to extend locally into stems, followed by interstem ordering and the subsequent development of aggregates into greater axial length. The stem length of the orientationally ordered structure formed in solution is typically longer than that in the vapor case by a factor of 2 to 3. It hence appears that although all previous MD results generally indicate that oriented aggregation is highly relevant to polymer nucleation, there could be quantitative or even qualitative differences between results of solution-state calculations and those of previous vapor phase studies. Here we report MD results for systems comprising three 300-mer PE chains in 1,2,4-trichlorobenzene (TCB) solution (ca. 6.5 wt % in concentration) at different temperatures, emphasizing the structural evolution and its T_c dependence for embryos formed up to 15 ns in crystallization time (t_c). Comparison with the standard model and the more recent theoretical[3] or empirical[13] models of primary nucleation is conscientiously made.

Method. The PE/TCB solution system basically contains 2000 TCB molecules and three 300-mer PE chains; this corresponds to a semidilute (ca. 6.5 wt %) solution. Commercial package Accelrys Material Studio was used for initial system generation (Amorphous Cell) and MD simulation engines (Forcite). United-atom potential (in the form of DREIDING force field[14]) was adopted for each methylene or methyne group, with a cutoff distance of 1.25 nm. To build the initial state, the PE chains are stochastically generated from the rotational isomeric state (RIS) model, whereas solvent molecules were randomly placed. The initial system density was set to 1.0 g mL^{-1}, followed by tuning the length of system box. After geometry optimization and an MD prerun of 500 ps at 300 or 400 K in the isobaric−isothermal (NPT) ensemble in steps of 2 fs, the system converged (i.e., < 1% in temperature fluctuations) to a stabilized density of ca. 1.1 g mL^{-1} with the MD box size decreased to 8 × 8 × 8 nm^3. Long-term MD runs up to t_c = 15 ns (i.e., 7.5×10^6 MD steps) were then performed for trajectory collection at different T_c. In one particular run, the MD system was doubled to 16 × 8 × 8 nm^3 to include six 300-mer PE chains and 4000 TCB molecules to demonstrate the coalescence of precursors.

Results. Shown in Figure 1 are selected snapshots of the 6.5 wt % PE/TCB system at t_c = 1 to 15 ns and T_c = 400 or 300 K. For the case of T_c = 400 K, the nucleation process is observed to start from aggregation of PE segments to a
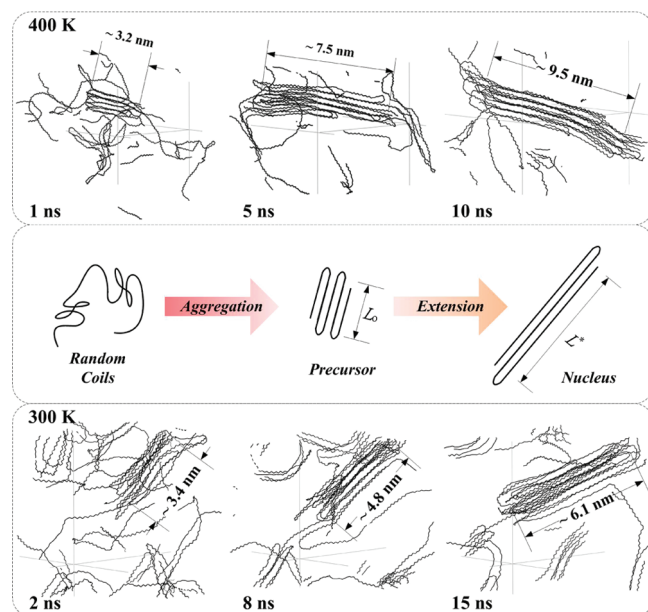
*To whom correspondence should be addressed.

Figure 1. Representative snapshots of the 6.5 wt % PE/TCB system at $t_c = 1$ to 15 ns and $T_c = 400$ (top) or 300 K (bottom) in an MD box $8 \times 8 \times 8 \text{ nm}^3$ in size. Only chain segments are shown, with TCB molecules hidden from the view. The middle frame recapitulates this single-precursor maturation process. Note that stems in the embryo may consist of segments from different chains.

Figure 2. Magnified vdW density cross sections of the incipient precursors comprising 17 (lower left, $T_c = 300$ K) or 14 (upper left, $T_c = 400$ K) irregularly aggregated stems of axial length $L_o \approx 3$ nm and the subsequently stabilized nucleus comprising 22 more fully packed stems (lower right, $T_c = 300$ K) of axial length $L^* \approx 6$ nm or 20 stems (upper right, $T_c = 400$ K) of axial length $L^* \approx 10$ nm. For $T_c = 300$ K, folds are highlighted in blue or magenta in the snapshots and indicated as dotted lines for the vdW density cross sections, whereas dangling celia are left unhighlighted. Even in this deep-supercooling case, adjacently re-entered stems constitute more than half of the population, albeit with significant presence of both nonadjacently re-entered stems and stems with dangling celia.

precursor of axial length $L_o \approx 3$ nm and comparable lateral size W_o at $t_c \approx 1$ ns. Note that there are similar aggregates of loose structure that emerge and dissipate transiently (cf. Figure S1, Supporting Information, SI), consistent with the classical picture of nucleation via density fluctuation. This is then followed by an extension stage where connecting segments are reeled in to join the stems in the embryo, resulting in an increase in axial length upon reorganization to $L^* \approx 10$ nm, which then remains largely unchanged beyond $t_c \approx 9$ ns with concomitant stabilization of total potential energy of the system (cf. Figure S2, SI). The stabilized embryo with axial length L^* hence operationally defines the critical nucleus size that is practically measurable. Note that the lateral size increases only modestly to $W \approx 3$ nm during the nucleation period. Experimentally, $T_m°$ of PE in 10% (w/v) TCB solutions should lie slightly above 135 °C (at which dissolution of a high molecular mass PE fraction was incomplete).[15] This suggests a still fairly respectable level of supercooling ($\Delta T \approx 8$ K) at the present concentration level of 6.5 wt %, consistent with the clear tendency toward aggregation at 400 K (127 °C) observed here. A generally similar process is observed in the more deeply supercooled case of $T_c = 300$ K, although it is slower in dynamics because of decreased thermal energy. The incipient axial length of the embryo (at $t_c \approx 2$ ns) remains the same at $L_o \approx 3$ nm; however, the final nucleus (beyond $t_c \approx 11$ ns) is significantly shorter in axial dimension ($L^* \approx 6$ nm) as compared with the 400 K case.

Aggregated embryos are generally poor in positional order, as demonstrated by magnified vdW density cross-sections in Figure 2. In the incipient precursor stage, the interstem distances are fairly large in spread (0.39 to 0.61 nm), with obtuse angles formed among neighboring methylene groups ranging from 113 to 134°, although orientational order of the stems is apparent. The features of oriented stems approximately equal in axial length and liquid-like lateral packing render the structure smectic-like (i.e., disk-like aggregates of stems with nematic-like orientational order) and certainly far
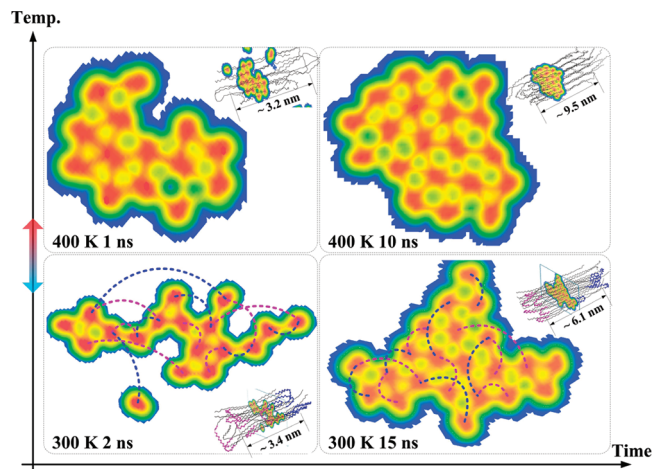
from crystalline. In the stabilized nucleus stage, the packing of stems is improved with peripherial area decreased, bringing interstem distances to a narrower range of 0.38 to 0.55 nm but obtuse angles to a wider spread of 108° to 144° and hence may be categorized as a distorted orthorhombic structure of PE.

Given in Figure 3 are representative snapshots during the extension stage, which involves reeling-in of further segments and axial translation of stems. For axial translation of a stem strongly adsorbed on an exposed (110) plane of PE crystal, the vdW barrier is estimated to be 8 kJ mol^{-1} of ethylene repeats via molecular mechanics calculations (cf. Figure S3, SI); this corresponds to ca. 200 to 300 kJ mol^{-1} for stems 6 to 10 nm in length. The values are approximately doubled for a stem lying within an exposed (110) plane and tripled if the stem is buried within the crystal. Such high barrier values (possibly overestimated because of the assumed crystalline packing as distorted or loosen packing may result in less friction, but the order of magnitude should remain valid) suggest a kinetic attribution that the critical dimension L^* is limited by interstem friction as the embryonic structure becomes compacted. As the barrier reflects interstem vdW attractions, this is consistent with the standard thermodynamic model where the free energy of fusion $\Delta g_f(T_c) \approx \Delta H_f° \Delta T / T_m°$ is considered, except that both $T_m°$ and $\Delta H_f°$ should correspond to the distorted orthorhombic structure of the nucleus. As the fold structure varies from loose loops to tight folds, adjacently or nonadjacently re-entered (cf. Figure 2), the fold surface energy (σ_e) may deviate significantly from the tight-fold limit (generally accepted[5] to be ca. 90 mJ m^{-2} for orthorhombic PE). In addition to the single-precursor maturation, there can be an alternative route of embryo maturation. As shown in Figure 4, two nearby precursors may sometimes coalesce into a single embryo via Brownian diffusion and oriented attachment, with concomitant extension of the axial length. The final nucleus size, however, is still determined by friction of stem translation as L^*. This coalescence route is expected to be of
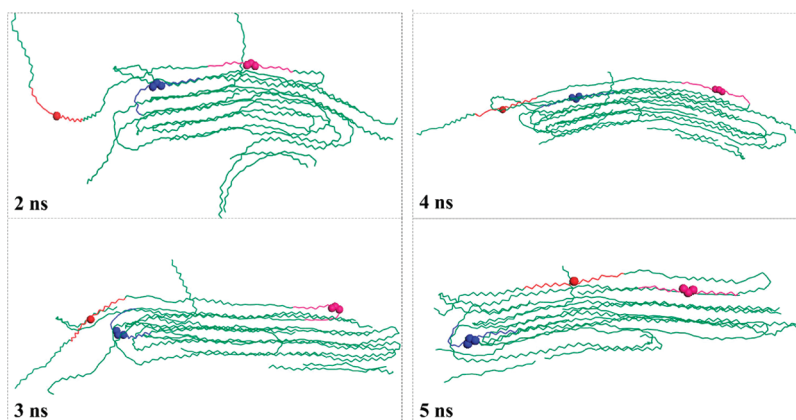
Figure 3. Representative snapshots in the extension stage of nucleation at 400 K. Highlighted red segments demonstrate reeling-in of new segments from left of view (t_c = 2 to 3 and 4 to 5 ns) or tightening of a loose fold (blue segments, t_c = 3 to 4 ns) for extension of the top two stems via axial translation of stems. Note that trajectories of the red and the blue triads (t_c = 2 to 3 ns) indicate adjacently and a nonadjacently re-entered folds, respectively.
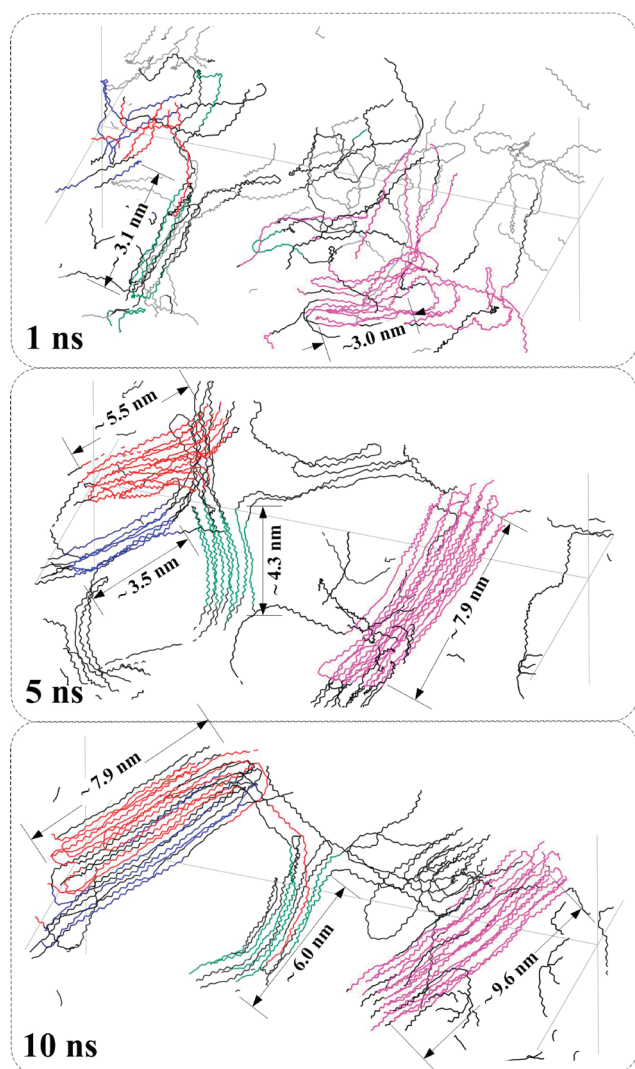

Figure 4. Representative snapshots at T_c = 400 K and t_c = 1 to 10 ns for a doubled MD box size of $16 \times 8 \times 8$ nm³ with 6 PE chains and 4000 TCB molecules. Four precursors (highlighted in red, blue, green, and magenta) can be seen at t_c = 5 ns; among them, the two (red and blue) near the upper left corner of view subsequently coalesce via Brownian diffusion and oriented attachment into a single precursor with concomitant extension of the axial length to 8 nm. The other two precursors (green and magenta) undergo simple extension to reach axial lengths of 6 and 10 nm, respectively.

increasing significance with increasing polymer concentration. We note that coalescence of nanograins via Brownian diffusion and (perfectly or imperfectly) oriented attachment, first observed by Métois et al.[16] nearly 4 decades ago, is now recognized[17,18] as a major process in the development of nanocrystalline materials. In view of the similarity in the nucleation process and the evolution time scale for both the normal ($8 \times 8 \times 8$ nm³) and the enlarged ($16 \times 8 \times 8$ nm³) systems, the basic features of segmental aggregation and subsequent extension via axial translation appear to be insensitive to system size. In addition, similar scenarios have been consistently observed from MD computations spanning wide concentration and temperature ranges.

Summarized schematically in Figure 5 are scenarios that the nucleation of PE in solution starts from segmental aggregation into incipient precursors of axial length L_o and comparable lateral size W_o. This is followed by single-precursor extension via reeling-in of new segments and axial translation of stems, reaching the critical size of L^* due to limited thermal energy to overcome the friction of axial translation. Alternatively, nearby precursors may coalesce via Brownian diffusion and oriented attachment, with concomitant axial readjustments to reach L^* and a slight increase in lateral width W. Strictly speaking, the nucleation process ends here; further stem attachment would correspond to crystal growth. Note that the designations of incipient aggregation time (t_o) and maturation time (t^*) may be more quantitatively made by examining the evolution of the corresponding radial distribution function (RDF, cf. Figure S4, SI).

Experimental observations are usually made on a macroscopic time scale far beyond this point; however, as long as the observations made do not incorporate effects from the much slower lamellar thickening process (i.e., within $t_c \approx 10^2$ s in the typical T_c range of PE),[19] the term "nucleus" is practically legitimate. Although demonstrated here only for the case of a 6.5 wt % PE solution, results of more extensive MD calculations indicate that the characteristic dimension $L_o \approx 3$ nm of incipient precursors is insensitive to increasing concentration up to the undiluted melt state, implying that L_o is closely related to chain rigidity at a fairly local level and intersegmental vdW attraction toward aggregation. In the deep-supercooling limit, extension of incipient precursor is limited because of decreased thermal energy (especially when the glass-transition temperature, T_g, is approached);[20] hence L_o serves as the lower bound of nuclear length L^* and should correspond to the empirical parameter
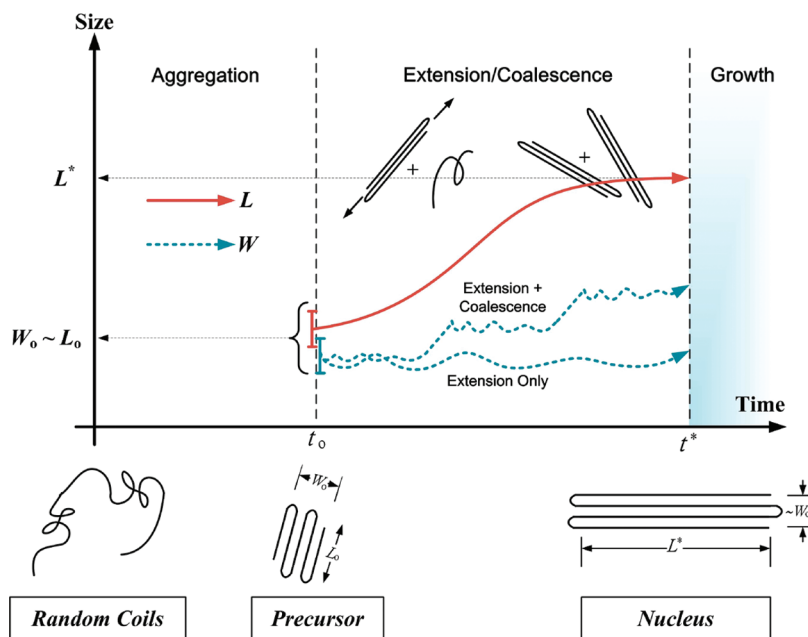
Figure 5. Schematic illustration of the nucleation process from random coils in solution, with L and W representing respectively the axial and the lateral dimensions of the aggregated embryos. The incipient precursor is characterized by an initial axial length L_o significantly shorter than the critical axial length L^* of fully developed nucleus. Note that L^* remains unaltered with prolonged MD time.

δ. In the cold-crystallization of glassy syndiotactic polystyrene ($T_g \approx 373$ K), the axial length of incipient embryos was found[2f] to be nearly constant ($l^* \approx 2.6$ nm) in a T_c range of 363 to 403 K (or $\Delta T = 204$ to 164 K with $T_m° \approx 567$ K).[22]

Discussion. The observed temperature-independence of L_o may be qualitatively understood via the following arguments. The critical aspect ratio for nematic order within the bundle-like aggregate in which volume fraction of stems $\phi_o \approx 1$ may be estimated to be $(L/D)_o \approx 4.5\phi_o \approx 4.5$ according to Onsager's mean-field theory[23] of nematic liquid crystals. This translates to $L_o \approx 2.2$ nm with stem diameter $D \approx 0.48$ nm, comparable to the observed $L_o \approx 3$ nm. The corresponding composition of the isotropic phase is $\phi' \approx 3.3 (L/D)_i^{-1} \approx 0.7$, significantly in excess of the concentration level here; hence the incipient embryo should be intrinsically unstable. With extension to the critical nucleus size of $L^* \approx 6$ to 10 nm for $T_c = 300$ to 400 K, we would expect $\phi' \approx 0.15$ to 0.10, much closer to the present concentration of 6.5 wt %. The ϕ' values here are certainly overestimated in view of the purely geometrical (volume exclusion) arguments in the Onsager theory compared with the present case of strong interstem vdW interactions. The key point here is that polymer aggregation starts with the formation of tufted aggregates that requires a nonvanishing characteristic length of chain extension.

As a final remark, we note that the prediction of diminishing nucleus size at the low-T_c extreme is not limited to the standard theory of polymer nucleation. Interested readers may have already noticed the morphological similarity between the present results and the "bundle" picture in the polymer nucleation theory proposed by Allegra et al.[3,24] However, there is an important difference. In Allegra's bundle model, a hexagonally packed embryonic structure was assumed for simplicity. This neglect of structural variations (from incipient embryos as loosely packed aggregates to distorted orthorhombic packing in the critical nucleus) still results in the prediction of diminishing nucleus dimension l^* at the low-T_c extreme. Our emphasis here is the evolution of kinetically determined embryonic structure of mesomorphic order throughout the primary nucleation

process: only with the continuous structural evolution in mind can the nonvanishing critical nucleus size in the far-from-equilibrium limit be understood.

Supporting Information Available: Transient emergence and dissipation of an aggregate, total potential energy evolution profiles of the PE/TCB system, relative vdW energy profiles for axial translation of a 10-mer stem, difference RDF profiles of the PE/TCB system, and RDF of a PE crystallite. This material is available free of charge via the Internet at http://pubs.acs.org.

References and Notes

(1) Wunderlich, B. *Macromolecular Physics*, Vol. *2*; Academic Press: New York, 1976; Ch. 5.
(2) Hoffman, J. D.; Davis, G. T.; Lauritzen, J. I., Jr. In *Treatise in Solid State Chemistry*, Vol. *3*; Hannay, N. D., Ed.; Plenum: New York, 1975; Ch. 7.
(3) Allegra, G.; Meille, S. V. *Adv. Polym. Sci.* **2005**, *191*, 87–135.
(4) Weber, C. H. M.; Chiche, A.; Krausch, G.; Rosenfeldt, S.; Ballauff, M.; Harnau, L.; Göttker- Schnetmann, I.; Tong, Q.; Mecking, S. *Nano Lett.* **2007**, *7*, 2024–2029.
(5) Hoffman, J. D.; Miller, R. L. *Polymer* **1997**, *38*, 3151–3212.
(6) Sumpter, B. G.; Noid, D. W.; Wunderlich, B.; Cheng, S. Z. D. *Macromolecules* **1990**, *23*, 4671–4677.
(7) Kavassalis, T. A.; Sundararajan, P. R. *Macromolecules* **1993**, *26*, 4144–4150.
(8) Fujiwara, S.; Sato, T. *J. Chem. Phys.* **1997**, *107*, 613–622.
(9) Guo, H. X.; Yang, X. Z.; Li, T. *Phys. Rev. E* **2000**, *61*, 4185–4193.
(10) Welch, P.; Muthukumar, M. *Phys. Rev. Lett.* **2001**, *87*, 218302.
(11) Muthukumar, M. *Adv. Polym. Sci.* **2005**, *191*, 241–274.
(12) Fujiwara, S.; Hashimoto, M.; Itoh, T.; Nakamura, H. *J. Phys. Soc. Jpn.* **2006**, *75*, 024605.
(13) Strobl, G. *Rev. Mod. Phys.* **2009**, *81*, 1287–1300.

(14) Mayo, S. L.; Olafson, B. D.; Goddard, W. A. *J. Phys. Chem.* **1990**, *94*, 8897–8909.

(15) Dorman, D. E.; Otocka, E. P.; Bovey, F. A. *Macromolecules* **1972**, *5*, 574–577.

(16) Masson, A.; Métois, J. J.; Kern, R. *Surf. Sci.* **1971**, *27*, 463–482.

(17) Shen, P.; Fahn, Y. Y.; Su, A. C. *Nano Lett.* **2001**, *1*, 299–303.

(18) Zhang, J.; Huang, F.; Lin, Z. *Nanoscale* **2010**, *2*, 18–34.

(19) Barham, P. J.; Keller, A. *J. Polym. Sci., Part B: Polym. Phys.* **1989**, *27*, 1029–1042.

(20) Cheng, S. Z. D. *Nature* **2007**, *448*, 1006–1007.

(21) Su, C. H.; Jeng, U.; Chen, S. H.; Lin, S. J.; Wu, W. R.; Chuang, W. T.; Tsai, J. C.; Su, A. C. *Macromolecules* **2009**, *42*, 6656–6664.

(22) Su, C. H.; Jeng, U.; Chen, S. H.; Cheng, C. Y.; Lee, J. J.; Lai, Y. H.; Su, W. C.; Tsai, J. C.; Su, A. C. *Macromolecules* **2009**, *42*, 4200–4207.

(23) De Gennes, P.-G.; Prost, J. *The Physics of Liquid Crystals*, 2nd ed.; Oxford University Press, Oxford, U.K., 1993; pp 59−63.

(24) Allegra, G.; Famulari, A. *Polymer* **2009**, *50*, 1819–1829.